JTE HCM-UTE
ISSN: 2615-9740

JOURNAL OF TECHNICAL EDUCATION SCIENCE
Ho Chi Minh City University of Technology and Engineering
Website: https://jte.edu.vn
Email: jte@hcmute.edu.vn

Estimate Effects of Reinforced Plain 2D-Woven Fabric Crimp on Elastic Constants of Geo-Composite by Analytical Models

Thanh Nhan Phan
Ho Chi Minh City University of Technology and Engineering, Vietnam

Corresponding author. Email: nhanpt@hcmute.edu.vn

ARTICLE INFO

Received:	23/03/2025
Revised:	13/05/2025
Accepted:	17/11/2025
Online First:	10/03/2026
Published:	28/11/2026

KEYWORDS

2D-woven fabric crimp;
Elastic mechanical properties;
Unit cell modeling;
Geo-composite;
Stiffness and compliance averaging;
Analytical models.

ABSTRACT

One important aspect influencing the mechanical properties of the composite material is thought to be the undulation of the fiber bundles in the woven fabric structure, which is employed as the reinforcing phase for the composite plate with geo-polymer resin. The unidirectional, straight, non-corrugated thread in the composite material system behaves mechanically differently from the fabric that is created during the weaving process. Furthermore, the mechanical properties of composite materials are also greatly influenced by the interaction between the fiber and matrix. Thus, it is important from a scientific and practical standpoint to assess how the parameters that define the corrugated fabric affect the elastic mechanical properties of composite plates and the reciprocal interaction between the fiber and matrix. Developing a mathematical model and computation technique to estimate the effects of reinforced plain 2D-woven fabric crimp on elastic constants of geo-composite and investigating adhesion between geo-polymer and fiber are the main goals of this paper. The simulation's findings indicate that the geo-composite panels reinforced with plain woven fabrics and very small crimped have a negligible effect on the materials' elastic constants. These outcomes also align with the experimental results.

DOI: https://doi.org/10.54644/jte.2026.1855

Copyright © JTE. This is an open access article distributed under the terms and conditions of the Creative Commons Attribution-NonCommercial 4.0 International License which permits unrestricted use, distribution, and reproduction in any medium for non-commercial purpose, provided the original work is properly cited.

1. Introduction

A composite plate (or laminate) is often constructed by stacking and bonding a number of fiber laminas (or plies) in the available thickness. Intuitively, it can be seen that the strength and stiffness of a laminate will depend on: elastic modules, stacking position, thickness, orientation angle of fiber laminas, and types of resin. One fiber-reinforced lamina in a laminate has usually two phases: continuous fibers (reinforcement phase) and binder compounds (matrix phase). As usual, matrix materials are considered a homogeneous phase, while the yarns (or strands) inside can align straightened (non-woven) or assembled into fabrics such as 2D-woven fabrics formed by interlacing yarns, knitted by interlooping yarns, and braided by intertwining yarns (Figure 1). The 2D fabrics typically have thicknesses very smaller than widths and lengths, while the 3D fabrics thickness is significantly thicker [1], [2].

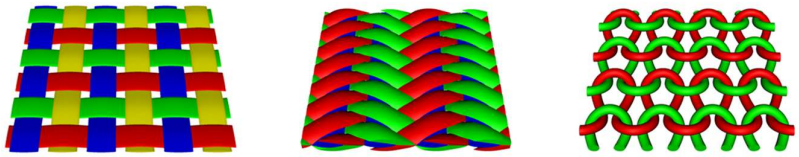

Figure 1. *2D-Fabrics: a. Woven fabric; b. Braided fabric; c. Knitted fabric.*

The mechanical properties of woven textiles are less evident than those of non-woven (angle-ply) laminates, even though they facilitate the creation of complex geometries. For this reason, woven fabrics are being researched for an increasing number of applications. The most popular textile method for the usage of composite plates is 2D-woven fabrics because they simplify the creation of intricate geometries.

The warp and weft strands, two sets of yarns that are interlaced orthogonally, define the woven structure. The weft thread travels perpendicular to the warp direction, and the warp strands exit the loom aligned with the direction of the cloth. Figure 2 depicts some of the simplest weave structures. The most common weaving structure shown in this image is plain weaving.

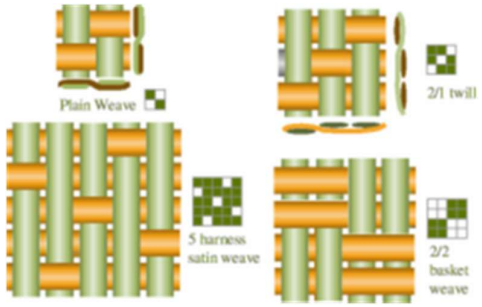

Figure 2. *Four most common weave structures.*

Researching the impact of fabric undulation on the elastic mechanical characteristics of composites has received more attention recently. Using finite element analysis of unit cell models, the influence of yarn cross-sectional shape and weft yarn crimp on the stiffness, static strength, and fatigue strength of carbon/epoxy 3D woven composite were investigated [2]. The results indicated that the early and final failure strengths of yarns with sharp edges were lower than those of yarns with smooth edges. Compared to the non-crimped composite, the crimped composite has a 10.12% lower Young's modulus in the weft direction. Through trials, some researchers studied how textile architecture and crimp affected the stiffness and strength of composites with 3D reinforcement [3]. A thorough experimental investigation of how pick density affects mechanical characteristics like tension, compression, short beam shear, and Izod impact energy in three-dimensional layer-to-layer glass/epoxy woven composite structures are presented [4].

Several analytical methods have been developed to predict the mechanical properties of 2D-woven textile composites using unit cells or representative volume elements (RVEs). Leading works on this subject include those [5], [6]. Based on stiffness averaging and rigidity ratio, some papers were able to control a two-orthogonal set of fabric compositions, such as laminate, with two laminae positioned at 0/90 places [7], [8]. For predicted expansion, scientists employed a variety of models, including the mosaic model (non-crimp) and the crimp model (where trigonometric functions were utilized to describe the undulation geometry and fiber continuity). Using the traditional laminate plate theory, rectilinear and sinusoidal crimp models to forecast expansion structures were created [9], [10]. In account of the corrugated yarn factor, a novel geometrical method to predict the elastic stiffness characteristics of 2D and 2.5D woven interlock composites have recently created [11]. The results of the analysis were verified by comparison with other models created in the literature and published articles. The correctness of the outcomes from the suggested models was assessed by numerical analysis. Under tensile stress, the mechanical properties and damage evolutions of carbon/epoxy woven fabric composites with three distinct geometries (one plain weave and two twill weave patterns) were investigated [12]. The findings demonstrated that the three composites with distinct crimps exhibit notable differences in the stress-strain curve, Poisson's ratio, residual strain, and strain map. A novel analytical model was presented predicting the in-plane shear modulus of plain-woven fabric composites with T300/Cycom970 fibers and a plastic matrix using experimental data as input [13]. The impact of the fiber volume fraction and crimp ratio on the in-plane shear modulus is examined in this study. In addition to successfully addressing the difficulties associated with analyzing the mechanical properties of plain-woven fabric composites, this model offers useful references for estimating parameters, building models, and designing experiments for other woven composite materials. Epoxy composites reinforced with textiles woven from hemp, a natural material, in a variety of weave styles were researched [14]. According to the results, plain weave fabric composites have lower tensile and flexural moduli than unidirectional fabric composites. Yarn angle and crimp are the primary causes of this alteration. The mechanical characteristics and failure behavior of aramid/epoxy laminated composites with plain and twill weaves

were investigated [15]. Finding out how fabric weaving patterns affect the laminated composites' mechanical performance is the goal of this study. The mechanical performance of twill fabric reinforced composites is superior to that of plain fabric composites, according to test results. Because of the floating length, the twill fabric composites produced a homogenous resin impregnation and a low crimp percentage. On the other hand, the high crimp percentage and irregular matrix impregnation at the interlacement zone of plain fabric composites result in poor mechanical performance.

Up till now, an excessive number of polymer-composite models have been used to investigate the microstructures and mechanical performance of laminate composites [2]-[15]. Nevertheless, there aren't many physical models or methods that can precisely predict the mechanical properties and behavior of geo-polymer-composite materials. Geo-polymers are new inorganic polymeric materials that resemble ceramics in appearance and chemical makeup but lack a distinct crystalline structure. They continue to be regarded as novel cement for concrete, a novel binder for fiber composites, and a novel substance for coatings and adhesives. Geo-polymer materials possibly fabricate composite materials not only with excellent mechanical properties such as lightweight and high strength in compression but also with ideal fire resistance (can sustain temperatures up to with long term exposure), low shrinkage, low thermal conductivity, nontoxic fumes and smokes, and resisting all inorganic solvents (only affected by strong hydrochloric acid) [16]. The mechanical characteristics of geo-polymer materials and their fiber bonding are entirely distinct from those of polymer materials. This article will examine and evaluate how the undulation of the reinforcement fabric affects the geo-composite plate's elastic constants. The plate is composed of three different fabrics: carbon, basalt, and E-glass and geo-polymers. An alternate approach that concentrates on creating a mathematical model and computation method is also presented in this work. The paper also examines the effects of the link between geo-polymer materials and three different fiber types on the mechanical characteristics of geo-composite materials.

2. Materials and Experimental Methods

2.1. Materials

Alumino-silicate powder (49 wt.%), alkali activator with NaOH/KOH (44.12 wt.%), and metakaolin powder (6.88 wt.%) from the Research Institute of Inorganic Chemistry Inc. in the Czech Republic were combined to create the geo-polymer binder. After giving the mixture a thorough stir, it was refrigerated for a full day. To create samples compression tests, geo-polymer binder was then poured into casts (ASTM-D790-03) [17]. As exemplary fabrics for the composite development, plain woven fabrics made of carbon, E-glass, and basalt have been used (Figure 3). In accordance with EN ISO 13934 [18], fabric samples for tensile testing were cut in both the warp and weft orientations. Tables 1 and 2 show the geo-polymer's and the fabrics' mechanical and physical characteristics.

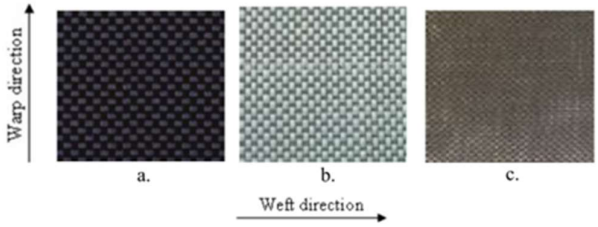

Figure 3. *Plain woven fabrics: a. Carbon; b. E-glass; c. Basalt.*

Table 1. *Physical and mechanical properties of geo-polymer.*

Physical and mechanical properties	Values
Density after curing and drying ρ_m (g/cm^3)	2.0 ± 0.01
Elastic modulus in compression, E (GPa)	11.7 ± 0.2
Shear modulus, G (GPa)	5.6 ± 0.2
Poisson's ratio, v	0.05 ± 0.01

Table 2. *Physical and mechanical properties of fabrics.*

Physical and mechanical properties	Values		
	Carbon fabric	**E-glass fabric**	**Basalt fabric**
Density of fiber ρ_f (g/cm^3)	1.65 ± 0.02	2.57 ± 0.02	2.7 ± 0.02
Thickness (mm)	0.24	0.38	0.16
Area density of fabrics ρ_w (g/m^2)	200	486	200
Tensile module E (GPa)			
Warp direction	25.1 ± 0.1	19.6 ± 0.2	24.2 ± 0.2
Weft direction	25.3 ± 0.1	16.4 ± 0.1	23.2 ± 0.1
Poisson's ratio, v	0.27	0.22	0.30

2.2. Fabrication of tensile and in plane shear geo-composite specimens

To reach the required thickness of approximately 3 mm for tensile samples and 4 mm for in-plane shear samples, the textiles were manually filled with geo-polymer binder, stacked together in the same direction, and compacted by a roller. After being built, the fabric-reinforced geo-polymer composites were put in a vacuum bag and allowed to be cured for two hours at room temperature at 0.003 MPa. The samples were then allowed to cure in an air environment for 20 hours at room temperature after the bag was placed in a curing oven set to 70°C for two hours. For tension, rectangular samples of 15 × 220 mm^2 that were cut from a large plate were utilized. For in-plane shear tests, the butterfly-shaped (or V-shaped) samples, which have the middle cross-sectional dimension of 4 mm, will be installed on a testing machine and held in place by four Arcan fixture halves. For tension tests, real thickness measured once more are 3.18 ± 0.27 mm for samples of carbon fabric reinforced geo-composites (including 10 layers of carbon); 3.04 ± 0.35 mm for samples of E-glass fabric reinforced geo-composites (7 layers of E-glass); and 3.50 ± 0.12 mm for samples of basalt fabric reinforced geo-composites (15 layers of carbon). The samples employed in plane shear testing have middle cross section thicknesses of 4.47 mm for carbon geo-polymer composite, 3.73 mm for E-glass geo-polymer composite, and 4.63 mm for basalt geo-polymer composite (Figure 4).

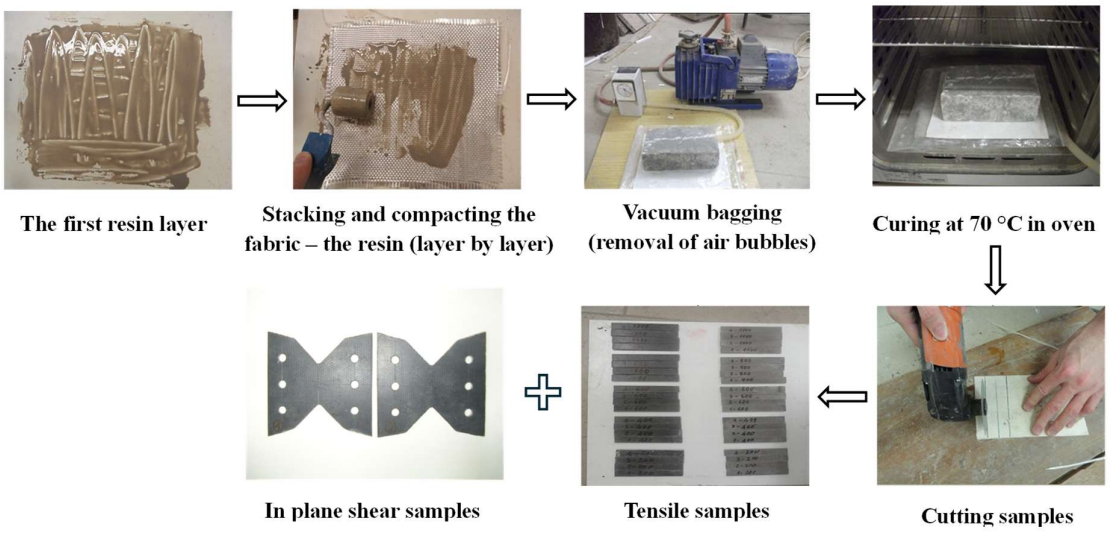

Figure 4. *Schematic diagram of the fabrication and cutting of the geo-composite.*

2.3. Measurements of the volume fractions of fabric, matrix and void in geo-composite

The densities and the volume fractions of fabric, matrix and void (or porosity) are estimated in fabric reinforced geo-composites by using the following equation:

$$\rho_c = \frac{m_c}{tLb}\ ;\quad V_f = \frac{n\rho_w}{t\rho_f}.100\%\ ;\ V_m = \frac{1}{t\rho_m}\left(\frac{m_c}{Lb} - n\rho_w\right).100\%\ ;\ \ V_v = 100 - (V_f + V_m) \tag{1}$$

where ρ_c is the density of geo-composites (g/cm^3); V_f, V_m, V_v are the volume fractions of fabric, matrix and void in the geo-composites (%); n is the number of fabric layers in the composite samples; m_c, t, L, b are the mass, thickness, length and width of the composite specimens (g), (mm), respectively; ρ_w is the density of fiber layer (g/m^2); ρ_f is the density of a single fiber (g/m^3); ρ_m is the density of matrix (g/m^3). All fraction results are the average of measurements from five samples.

The estimate results of densities and volume fractions of fabric, matrix and void in three types of geo-composite cured temperature fixed at 70°C for 24 h are shown in Table 3.

Table 3. *The densities and volume fractions of fabric, matrix and void of geo-composites.*

The parameters	Values		
	Carbon geo-composite	**E-glass geo-composite**	**Basalt geo-composite**
The densities, ρ_c (g/cm^3)	1.51 ± 0.02	1.97 ± 0.02	1.80 ± 0.02
The volume fractions of fabric, V_f (%)	39.4 ± 0.5	41.1 ± 0.3	40.3 ± 0.7
The volume fractions of matrix, V_m (%)	40.5 ± 0.8	37.3 ± 0.2	45.3 ± 0.6
The volume fractions of void, V_v (%)	20.1 ± 0.2	21.6 ± 0.2	14.4 ± 0.1

2.4. Measurements of mechanical properties of geo-composite

Tensile testing and in-plane shear testing are two sets of experiments used to determine the mechanical properties of geo-composite materials. To find the directional Young's moduli and strength using the standard ASTM C 1275-00 [19], geo-composites samples (3 × 15 × 220 mm^3) were tested for tension in both the warp and weft directions using the universal tester TIRA test 2810 (Germany). The maximum failure load and experimentally determined elongation were used to calculate the stress, strain, and modulus of elasticity in the tensile tests, as shown below.

$$\sigma = \frac{F}{bt}\ ;\ \varepsilon = \frac{\Delta L}{L}\ ;\ E = \frac{\Delta\sigma}{\Delta\varepsilon} \tag{2}$$

where σ is tensile stress (MPa); ε is tensile strain, F is tensile force (N); t, L, b are the thickness, length and width of the composite specimens (mm); ΔL is elongation of the composite specimens; E is elasticity modulus of geo-composite material (GPa); $\Delta\sigma/\Delta\varepsilon$ is the ratio of stress difference and strain difference measured at the linear segment of the graph.

The in-plane shear characteristics of the geo-composite are measured using a series of V-shaped notched samples. The specimens were placed on the testing machine TIRA test 2810 (Germany) and held in place by four Arcan fixture halves. The strain field of the specimens was examined using a single DIC camera from Dantec Dynamics Company. Every test was conducted at room temperature (20–25 °C) with a relative humidity of roughly 70%, and at the same loading speed of 1 mm/min. While the Q-400 camera system can optically identify the plane shear strain of a specimen's center region, plane shear stress can be quantified using loads recorded from a testing machine's load cell. The optical apparatus was configured to capture one image every second. Both testing machine and the optical device were synchronized together. Hence the magnitude of shear stress and shear modulus was calculated as follows:

$$\tau_{xy} = \frac{F}{bt}\ ;\ G = \frac{\Delta\tau}{\Delta\gamma} \tag{3}$$

where τ_{xy} is plane shear stress (MPa); F is shearing force (N); t, b are the thickness and width of the V-shaped notched samples (mm); G is shear modulus of geo-composite material (GPa); $\Delta\tau/\Delta\gamma$ is the ratio of stress difference and strain difference measured at the linear segment of the graph.

Table 4 shows tensile and shear mechanical properties of three types of geo-composites.

Table 4. *Tensile and shear mechanical properties of three types of geo-composites.*

Mechanical properties		Values		
		Carbon Geo-composite	**E-glass Geo-composite**	**Basalt Geo-composite**
Tension in a warp direction	Tensile modulus, E (GPa)	12.6	9.6	10.2
	Tensile strength, σ (MPa)	191.4	76.3	35.8
	Tensile failure strain, ε (%)	2.40	3.19	1.75
Tension in a weft direction	Tensile modulus, E (GPa)	12.5	8.5	11.3
	Tensile strength, σ (MPa)	190.4	65.6	35.6
	Tensile failure strain, ε (%)	2.43	2.72	1.72
In plane shear	Shear modulus, G (GPa)	5.2	5.1	Failed
	Shear strength, τ (MPa)	6.5	3.8	Failed

3. Numerical and analytical models to predict elastic constants

Since every layer in the sample stacks with the same orientation in the composite material, one repeating unit cell of lamina is chosen to mimic mechanical and physical qualities. Two orthogonal yarn couplings are weaved and surrounded by a matrix in this rectangular parallelepiped unit cell reinforced plain woven fabric. assuming that there is an equal distribution of emptiness and matrix both inside and between yarns. In this instance, the matrix acts as an adhesive between filaments and yarns.

The unit cell's geometrical model as seen from the y-direction is shown in Figure 5. We must consider the general scenario in which the weft yarn (represented by index 2) and warp yarn (represented by index 1) have the same thickness (equal to half of the lamina thickness) but different geometrical features. It is feasible to speculate that each yarn in a unit cell is made up of two arcs with the same radius but pointing in opposing directions; two systems of warp and weft yarns overlap ideally since the thickness and pitch of the fabric are relatively small. Consequently, it is presumed that the strands' cross section is lenticular.

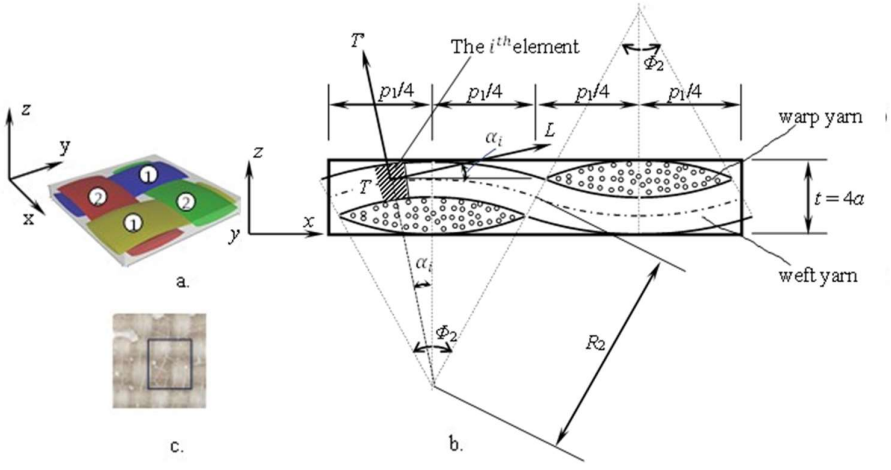

Figure 5. *a. The unit cell; b. Geometrical model of the unit cell (view from y-direction); c. Geo-composite sample (view from z-direction).*

In the unit cell's geometrical model, warp and weft yarns' pitch of p_1 and p_2 and thickness of $t = 4a$ are known among the characteristics. These primary parameters will be used to determine the remaining parameters, which are ascertained as follows.

The angles of the warp and weft yarn arcs are:

$$\emptyset_1 = 2\,arcsin\left(\frac{2p_2t}{p_2^2+t^2}\right),\ \emptyset_2 = 2\,arcsin\left(\frac{2p_1t}{p_1^2+t^2}\right) \tag{4}$$

The warp and weft yarn axis lengths are:

$$l_1 = \frac{(p_2^2+t^2)\emptyset_1}{4t},\ l_2 = \frac{(p_1^2+t^2)\emptyset_2}{4t} \tag{5}$$

The cross sections' areas of the warp and weft yarns are:

$$A_1 = \left(\frac{p_1^2+t^2}{8t}\right)^2.(\emptyset_2 - sin\,\emptyset_2),\ A_2 = \left(\frac{p_2^2+t^2}{8t}\right)^2.(\emptyset_1 - sin\,\emptyset_1) \tag{6}$$

The warp and weft yarns' crimps are denoted by c_1 and c_2 and determined:

$$c_1 = \frac{l_1}{p_2} - 1 = \frac{(p_2^2+t^2)\emptyset_1}{4p_2t} - 1,\ c_2 = \frac{l_2}{p_1} - 1 = \frac{(p_1^2+t^2)\emptyset_2}{4p_1t} - 1 \tag{7}$$

The model's total yarn volume fraction is denoted by V_y and detemined:

$$V_y = \frac{2(A_1l_1 + A_2l_2)}{p_1p_2t}.100\% \tag{8}$$

By using this geometrical model for geo-composites made of reinforced carbon, basalt, and E-glass, we can determine crucial parameters such crimps, warp and weft yarn arc angles, and the total yarn volume fraction, which are displayed in Table 5.

Table 5. *The basic geometrical parameters of geo-composites.*

The basic geometrical parameters		Values		
		Carbon Geo-composite	**E-glass Geo-composite**	**Basalt Geo-composite**
Thickness of unit cell, t (mm)		0.32	0.43	0.23
Pitches of	Warp yarn, p_1 (mm)	2.0	2.7	1.9
	Weft yarn, p_2 (mm)	2.0	2.3	1.9
Crimps of	Warp yarn, c_1	0.0170	0.0231	0.0097
	Weft yarn, c_2	0.0170	0.0168	0.0097
Arc angles of	Warp yarn, $\emptyset_1$ (deg)	36.38	42.48	27.62
	Weft yarn, $\emptyset_2$ (deg)	36.38	36.21	27.62
Total yarn volume fraction, V_y (%)		68.1	68.4	67.5

The unit cell model was created to consider the undulations and continuity of the fibers in a composite fabric. We must determine the elastic characteristics of unidirectional tows in the unit cell to compute the parameters of lamina reinforced woven fabrics. Next, we use either the compliance averaging approach or the stiffness averaging method for the unit cell in the lamina.

A yarn segment, which is regarded as a unidirectional rod, must have its elastic constants calculated to ascertain the elastic mechanical properties of a unit cell reinforced with woven fabric. Each unit cell

has four yarns and a corresponding volume fraction of matrix. One yarn is thought to contain numerous segments that connect to one another and have variable directions, which is the author's difference from previous research works. In a unit cell, the yarns are regarded as orthotropic, whereas the matrix that surrounds them is regarded as isotropic material. assuming a resin and fiber combination with excellent adhesion. Unidirectional lamina micromechanics theory can be used to calculate yarn mechanical properties [20].

The longitudinal elastic modulus of the yarn sections can be counted by the rule of mixtures [20]:

$$E_L = E_f V_f + E_m V_m + E_v V_v \tag{9}$$

The two transverse elastic moduli, $E_T = E_{T'}$, are given [20] as:

$$\frac{E_T}{E_m} = \frac{1 + \xi\eta V_f}{1 - \eta V_f} \tag{10}$$

The equation for the major Poisson's ratio, ν_{LT}, is obtained as follows [20]:

$$\nu_{LT} = \nu_f V_f + \nu_m V_m + \nu_v V_v \tag{11}$$

The equation for the shear modulus, G_{LT}, is [20]:

$$\frac{G_{LT}}{G_m} = \frac{1 + \xi\eta V_f}{1 - \eta V_f} \tag{12}$$

From equation (9) to equation (12), the elastic constants for a unidirectional yarn segment are determined in Table 6. Data from this table will be used to construct the unidirectional compliance and stiffness matrices $S_{yarn}^{(i)}$, $C_{yarn}^{(i)}$ for each yarn segment [20].

After describing geometry of the unit cell with consideration of the crimp parameters, we can apply the stiffness averaging method and the compliance averaging method for predicting elastic properties of unit cell in the following steps:

Table 6. *The elastic constants for a unidirectional yarn.*

The parameters	Values		
	Carbon Geo-composite	**E-glass Geo-composite**	**Basalt Geo-composite**
The longitudinal modulus in a warp direction, E_{L_warp} (GPa)	17.0	14.0	17.0
The longitudinal modulus in a weft direction, E_{L-weft} (GPa)	17.1	12.2	16.5
The transverse modulus, $E_T = E_{T'}$ (GPa)	13.8	11.9	12.6
The major Poisson's ratio, $\nu_{LT} = \nu_{LT'}$	0.16	0.13	0.13
The transverse Poisson's ratio, $\nu_{TT'} \approx \nu_m$	0.05	0.05	0.05
The shear modulus, $G_{LT} = G_{LT'}$ (GPa)	6.2	5.7	6.0
The transverse shear modulus, $G_{TT'} = \frac{E_T}{2(1+\nu_{TT'})}$	6.6	5.7	6.0

- Dividing every half of yarn in a unit cell into 10 yarn segments (n = 10). Each yarn element is a unidirectional composite (or a rod) with the same unidirectional compliance and stiffness matrices of $S_{yarn}^{(i)}$, $C_{yarn}^{(i)}$.

For elements belonging to the weft yarn system or to the warp yarn system, the general linear orthogonal coordinate transformation matrix of the local system (L, T, T') to the global system (x, y, z) to have a form (see Figure 5 again):

$$M_{weft}^{(i)} = \begin{bmatrix} cos(\alpha_i) & 0 & sin(\alpha_i) \\ 0 & 1 & 0 \\ -sin(\alpha_i) & 0 & cos(\alpha_i) \end{bmatrix} \quad (13)$$

$$M_{warp}^{(i)} = \begin{bmatrix} 0 & cos(\alpha_i) & sin(\alpha_i) \\ 1 & 0 & 0 \\ 0 & -sin(\alpha_i) & cos(\alpha_i) \end{bmatrix} \quad (14)$$

- Calculate the global compliance and stiffness matrices of the unidirectional yarn elements thanks to the strain and stress transformation matrices T_ε, T_σ:

$$S_{g-yarn}^{(i)} = T_\varepsilon . S_{yarn}^{(i)} T_\sigma^{-1} \; ; \; C_{g-yarn}^{(i)} = T_\sigma . C_{yarn}^{(i)} T_\varepsilon^{-1} \quad (15)$$

- To determine the overall compliance and stiffness matrices, volumetrically average the compliance and stiffness matrices of all unidirectional elements and the percentage of matrix between yarns S, C:

$$S = \sum_{i=1}^{10} (4k_{warp} S_{g_warp}^{(i)} + 4k_{weft} S_{g_weft}^{(i)}) + k_m S_{g-matrix} \quad (16)$$

$$C = \sum_{i=1}^{10} (4k_{warp} C_{g_warp}^{(i)} + 4k_{weft} C_{g_weft}^{(i)}) + k_m C_{g-matrix} \quad (17)$$

where: $S_{g-matrix}$, $C_{g-matrix}$ are the global compliance and stiffness of proportion of matrix between yarns and are independent on coordinate system.

k_{warp}, k_{weft} are the relative volumetric proportion of the warp and weft yarn sub-system in unit cell; k_m is the relative volumetric proportion of matrix between yarns in unit cell. k_{warp}, k_{weft} and k_m can be determined by equation (18).

$$k_{warp} = \frac{A_1 l_1}{20 p_1 p_2 t} \; ; \; k_{weft} = \frac{A_2 l_2}{20 p_1 p_2 t} \; ; \; k_m = 1 - 40(k_{\text{warp}} + k_{\text{weft}}) \quad (18)$$

here A_1, A_2, l_1, l_2 are referred from the equations (5), and (6).

From the compliance averaging approach, elastic properties are determined:

$$E_x = \frac{1}{S_{11}} \; ; \quad E_y = \frac{1}{S_{22}} \quad ; \quad \nu_{xy} = -\frac{S_{12}}{S_{22}} \quad ; \quad G_{xy} = \frac{1}{S_{66}} \quad (19)$$

Elastic characteristics are also obtained using the stiffness averaging method:

$$E_x = \frac{1}{S_{11}^*} \; ; \quad E_y = \frac{1}{S_{22}^*} \quad ; \quad \nu_{xy} = -\frac{S_{12}^*}{S_{22}^*} \quad ; \quad G_{xy} = \frac{1}{S_{66}^*} \quad (20)$$

where $S^* = (C)^{-1}$

To investigate the effect of reinforced plain 2D-woven fabric crimp on the elastic constants of geo-composite, we also need to build a cross-ply model (no crimp) with the same mechanical properties of the fiber and matrix and model dimensions. The identical method is used to obtain the elastic constants for this model; the only difference is that $\alpha_i = 0$ is substituted.

4. Results and Discussion

A code file is written by Matlab software to calculate the elastic constants of geo-composite. Table 7 displays the findings from the experiments and geo-composite models (woven fabric and cross-ply).

Overall, the results from the crimp model show that the crimp of the fiber bundles in the woven fabric has a negligible effect (decrease approximately 1%) on the mechanical properties of the composite panels. This can be explained by the fact that the crimp of the fiber bundles is very small to significantly affect the mechanical properties of the plain weave panels compared to the cross-weave panels. The undulation of carbon, E-glass and basalt fiber bundles in the plain-woven sheet can be found in Table 5 with an average difference of about 2% compared to the straight fiber bundles in cross weave sheet. Here, the undulation is reduced because of the very narrow cross-section of the fiber bundle, which causes very little bending. The average stiffness and average compliance methods used to determine the mechanical properties of composite panels produce distinctly different outcomes. This is explained by the fact that Poisson's ratio and elastic moduli are calculated when the complete unit cell is considered in a constant strain state (for the stiffness averaging method) or a constant stress state (for the compliance averaging method).

Table 7. *The elastic constants from experiments and the models.*

The elastic constants of geo-composite reinforced by fiber		Experiments	Woven fabric model		Cross-ply model	
			The averaging stiffness method	The averaging compliance method	The averaging stiffness method	The averaging compliance method
Carbon	E_x (GPa)	12.50	14.31	13.87	14.32	13.92
	E_y (GPa)	12.60	14.29	13.89	14.29	13.89
	ν_{xy}	----	0.12	0.11	0.12	0.11
	G_{xy} (GPa)	5.20	6.01	6.00	6.01	5.99
E-glass	E_x (GPa)	8.50	11.97	11.95	11.97	11.94
	E_y (GPa)	9.60	12.59	12.48	12.59	12.48
	ν_{xy}	----	0.10	0.10	0.10	0.10
	G_{xy} (GPa)	5.10	5.67	5.67	5.67	5.67
Basalt	E_x (GPa)	11.30	13.65	13.30	13.66	13.33
	E_y (GPa)	10.20	13.83	13.44	13.83	13.44
	ν_{xy}	----	0.09	0.09	0.09	0.09
	G_{xy} (GPa)	----	5.87	5.86	5.87	5.86

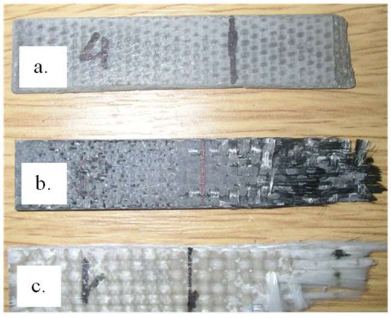

Figure 6. *Tensile failure of geo-composites with fabrics: a. Basalt; b. Carbon; c. E-glass.*

The experiment and the simulated outcomes still diverge greatly. This variance can be explained by the less-than-ideal adhesion between the matrix and the fiber, as well as the type of mechanical property change that takes place when the matrix material joins with the fiber material. The type of bonding

between the fiber and matrix in tensile samples of each geo-composite at failure is depicted in Figure 6. It is evident that the failure traces of basalt geo-composite and carbon and E-glass geo-composites differ greatly when samples are inspected in damaged places. The carbon reinforced fabric geo-polymer composite exhibits the matrix's good packing inside the fabric layers, but the E-glass fabric exhibits matrix geo-polymer debonding, which may be brought on by the absence of matrix geo-polymer impregnation in the fabrics. The basalt geo-composite's reinforcing fibers vanish at the location of damage, unlike bundles of carbon and E-glass fibers. In other words, the essential components used to carry loads are still the same for carbon and E-glass fabrics. In opposite, basalt fibers and geo-polymer may react chemically to make a homogenous substance that resembles ceramics.

4. Conclusion

The crimp of reinforced plain 2D-woven fabric has a negligible effect on the stiffness of geo-composite materials because the fiber bundle's cross-section is rather small, which causes the undulation to decrease. According to the unit cell's geometrical model, the average crimp of the warp and weft yarn in basalt, carbon, and E-glass fabrics is 2% higher than that of a straight fiber bundle. The relative volumetric fraction of each component in the unit cell can be used to calculate the elastic moduli and Poisson's ratio of geo-composite materials using average stiffness and average compliance approaches using mechanical properties of fiber and matrix components. Because of the imperfect adhesion between the matrix and the carbon and E-glass fibers, as well as the type of mechanical property change that takes place when the matrix material joins with the basalt fiber, the analytical results still deviate from the experiment. To further examine the overall crimp, more varied 2D-weave patterns should be used with this analytical model.

Acknowledgments

The authors would like to thank Ho Chi Minh City University of Technology and Engineering for supporting this study.

Conflict of Interest

The author declares no conflict of interest.

REFERENCES

[1] D. Ghlaim, "Woven factor for the mechanical properties of woven composite materials," *J. Eng.*, vol. 6, p. 4, 2010.
[2] S. Kari and M. Kumar, "Effect of yarn cross-sectional shapes and crimp on the mechanical properties of 3D woven composites," *Composites*, 2009, doi: 10.5281/zenodo.15457208.
[3] F. Stig and S. Hallström, "Effects of crimp and textile architecture on the stiffness and strength of composites with 3D reinforcement," *Adv. Mater. Sci. Eng.*, vol. 2019, no. 1, 2021, doi: 10.1155/2019/8439530.
[4] M. Dahale, G. Neale, and R. Lupicini, "Effect of weave parameters on the mechanical properties of 3D woven glass composites," *Compos. Struct.*, 2020, doi: 10.1016/j.compstruct.2019.110947.
[5] J. Whitcomb and J. Noh, "Evaluation of various approximate analyses for plain weave composites," *J. Compos. Mater.*, vol. 33, 1999, doi: 10.1177/002199839903302101.
[6] A. Bogdanovich and C. Pastore, *Mechanics of Textile and Laminated Composites*. London, U.K.: Chapman & Hall, 1996.
[7] T. Ishikawa and T. W. Chou, "Elastic behavior of woven hybrid composites," *J. Compos. Mater.*, vol. 6, pp. 2–19, 1982.
[8] T. Ishikawa and T. W. Chou, "Stiffness and strength behavior of woven fabric composite," *J. Mater. Sci.*, vol. 17, pp. 3211–3220, 1982.
[9] K. Saka and J. Harding, "A simple laminate theory approach to the prediction of the tensile impact strength of woven hybrid," *Composites*, vol. 21, pp. 439–447, 1990.
[10] J. Carey and M. Munro, "Longitudinal elastic modulus prediction of a 2-D braided fiber composite," *J. Reinf. Plast. Compos.*, vol. 22, pp. 813–631, 2003.
[11] A. K. Mohamad and R. Yafai, "New geometrical modelling for 2D fabric and 2.5D," *Textiles*, pp. 142–161, 2022.
[12] G. Zhou and Q. Sun, "Experimental investigation on the effects of fabric architectures on mechanical and damage behaviors of carbon/epoxy woven composites," *Compos. Struct.*, vol. 257, 2020, doi: 10.1016/j.compstruct.2020.113366.
[13] X. Jianxun, G. Weicheng, Z. Rui, and L. Guozeng, "An analytical model for the in-plane elastic shear modulus of plain-woven fabric composites and its application and experimental validation," *Text. Res. J.*, vol. 95, no. 15–16, 2025, doi: 10.1177/00405175241276815.
[14] N. S. Karaduman, "Experimental investigation of the effect of weave type on the mechanical properties of woven hemp fabric/epoxy composites," *J. Compos. Mater.*, vol. 56, no. 8, pp. 1255–1265, 2022.
[15] S. Sagar, X. Wang, K. Ali, and Y. Yang, "A study on the mechanical performance of aramid-epoxy laminated composites with plain and twill woven structure," in *Proc. 2022 Sino-Africa Int. Symp. Textile Apparel (SAISTA)*, Shanghai, China, 2022.
[16] S. Samala and N. P. Thanh, "Correlation of microstructure and mechanical properties of various fabric reinforced geo-polymer composites after exposure to elevated temperature," *Ceram. Int.*, vol. 41, pp. 12115–12129, 2015.
[17] ASTM D790-03, *Standard Test Methods for Flexural Properties of Unreinforced and Reinforced Plastics and Electrical Insulating Materials*.
[18] EN ISO 13934, *Textiles — Tensile Properties of Fabrics*.

[19] ASTM C1275-00, *Standard Test Method for Monotonic Tensile Behavior of Continuous Fiber-Reinforced Advanced Ceramics with Solid Rectangular Cross-Section Test Specimens at Ambient Temperature*.
[20] A. K. Kaw, *Mechanics of Composite Materials*. Taylor & Francis, 2006.

Thanh Nhan Phan received the B.S. degree in mechanical engineering from Nha Trang University, Khanh Hoa, Vietnam, in 1995 and the M.S. degree in mechanical engineering from Nha Trang University, Khanh Hoa, Vietnam, in 1998. He received Ph.D. in Liberec University of Technology (Czech) in 2014. Currently, he is a lecturer of Mechanical Engineering Faculty in Ho Chi Minh City University of Technology and Engineering (formerly Ho Chi Minh City University of Technology and Education). His research interest includes mechanics of composite materials, friction stir welding, and dynamics of multi-body system.
Email: nhanpt@hcmute.edu.vn. ORCID: https://orcid.org/0000-0002-5668-0135